Imaging of barely visible impact damage on a composite panel using nonlinear wave modulation thermography

Dimitrios Dionysopoulos, Gian Piero Malfense Fierro, Michele Meo, Francesco Ciampa*

Materials and Structures Centre (MAST), Department of Mechanical Engineering, University of Bath, Claverton Down, BA2 7AY, Bath, UK

*Email: f.ciampa@bath.ac.uk

Abstract

Thermosonics is a well-established non-destructive evaluation (NDE) technique that uses an infrared camera to visualise material damage by capturing the frictional heating at crack surfaces when the sample under inspection is vibrated. A high power ultrasonic horn is typically used to generate vibrations, which is pressed against the surface of the test component. However, the direct contact between the horn and the surface generates acoustic chaos and high-amplitude vibrations, which can lead to non-reproducible and unreliable measurements and, ultimately, they can harm the structural integrity of components. This paper proposes an alternative to thermosonics, here named as nonlinear wave modulation thermography, for the detection and imaging of material flaws on a damaged carbon fibre composite panel. This material inspection technology combines the concept of nonlinear wave modulation spectroscopy using dual excitation with contact piezoelectric transducers and thermographic equipment. Whilst nonlinear ultrasonic modulation was used to enhance the sensitivity to micro-cracks, an infrared camera was used for defect visualisation. A nonlinear narrow sweep excitation method was employed to experimentally identify the dual excitation frequencies that resulted in high-amplitude damage resonance effects causing frictional heat at crack surfaces. A laser vibrometry system was also used to create a spatial mapping of the amplitude of sidebands. Nonlinear

wave modulation thermography has proved to successfully detect barely visible impact damage in composites in a quick and reliable manner, thus overcoming the limitations of traditional optical thermography and thermosonics.

Keywords: Thermosonics, Thermography, Nonlinear Ultrasounds, Laser Vibrometry, Composites

1 Introduction

The drive for weight reduction and the need for materials of high strength and impact-resistance have led to the increased use of carbon fibre reinforced plastic (CFRP) composites in the aerospace industry. However, the assessment of composite materials is particularly challenging for low velocity impact damage, which is commonly referred to as barely visible impact defect (BVID). This material failure can be caused either at the manufacturing stage or during in-service and it can severely decrease the strength of composites thus leading to catastrophic failures. For critical components such as aircraft primary and secondary structures, non-destructive evaluation (NDE) techniques, such as ultrasounds, thermography and eddy currents, are necessary to guarantee that components are free of any harmful damage [1], [2], [3]. Active infrared (IR) thermography is a well-established NDE inspection technology for composites that uses external thermal excitation sources such as optical radiation [4], electromagnetic stimulation [5] and acoustic/ultrasonic waves [6] to generate heat in the component under inspection. Optical thermography uses optical flashes or heaters to heat the sample on its surface and then record the temperature decay curve using an infrared camera. However, the usage of external optical thermal sources may limit the image of defects within a few millimetres from the material surface. In addition, the lack of a significant air gap between micro-cracked surfaces may not generate any significant variation of the local temperature needed for damage detection. Thermosonics [7], also known as ultrasonic stimulated thermography or vibro-thermography, relies on the acoustic/ultrasonic excitation of the tested part using a high-power ultrasonic horn. In this

technique, material defects are visualised by observing the vibration-induced frictional heat with an IR camera. The primary sources of heat generation in a vibrating crack include frictional rubbing of crack surfaces, plastic deformations and viscoelasticity, which mainly depends on the test material, the type of defect and the applied vibrational stress level [8]. Experimental evidence has shown that 90-95% of frictional energy in sliding contacts is transformed into heat [9]. Crack surfaces would therefore experience larger temperature variations. This temperature raise would be transferred to the surface layers above the defect, thus allowing for damage detection. However, a major limitation of thermosonics is that the acoustic vibration generated by the horn tends to be "chaotic" and highly non-reproducible [10]. The exposure to high-power excitation generated by the horn may also further degrade the structural integrity of components.

The thermographic method presented in this paper, here named as nonlinear wave modulation thermography (NWMT), aims to increase the probability of defect detection and repeatability of thermosonics using nonlinear ultrasonic wave modulation and contact piezoelectric (PZT) transducers [11], [12]. In particular, by transmitting two periodic waves in the damaged material, i.e. a high- and low-frequency mode, the amplitude of both frequency components can be modulated due to the interaction of elastic waves with the material damage [13]. As a result of this interaction, new frequencies and associated modes known as higher harmonics (i.e. even and odd multiples) and sidebands (i.e. sum and differences) of the driving frequencies, can be generated [14]. Hence, the damage itself can act as a nonlinear mixer of the dual excitation frequencies [15], [16]. In an intermodulation experiment on a damaged composite sample using a low input frequency f_1 and a high frequency f_2 with amplitudes A_1 and A_2, respectively [17], a number of sidebands (e.g. f_2-nf_1 and f_2+nf_1, with n a positive integer number) were generated. Moreover, recent studies have highlighted the benefit of exciting the component under inspection at its damage-specific resonance frequency, also known as local defect resonance (LDR) [18], [19], [20]. Indeed, if the excitation frequency matches the damage resonance, the vibration amplitude of nonlinear elastic phenomena can be

increased. From a physical point of view, the clapping/rubbing of asperities of the two contacting crack surfaces vibrating at their resonance frequency generates high frictional heat at the damage location, which then leads to higher temperature variations across the defect. Such a temperature increase can then be recorded with an IR camera [21], [22]. Assuming that the internal structural flaw such as a delamination in a composite laminate of thickness h is represented by a flat bottom hole, i.e. a thin circular defect of radius r, the analytical expression of the LDR frequency f_d is [23]:

$$f_d \cong \frac{1.6d}{r^2}\sqrt{\frac{E}{12\rho\left(1-\upsilon^2\right)}}, \tag{1}$$

where E and ν are the effective elastic modulus and Poisson's ratio of the composite laminate, respectively, ρ is the density and d is the depth of the portion of volume below the defect. Eq. (1) corresponds to the first bending mode of a circular plate with clamped boundaries. For a quadratic-shaped defect with side length l, Eq. (1) becomes:

$$f_d \cong \frac{4\pi d}{3l^2}\sqrt{\frac{E}{6\rho\left(1-\upsilon^2\right)}}, \tag{2}$$

where B_s is the bending stiffness given by $B_s = Ed^3/12\left(1-\nu^2\right)$.

However, the experimental determination of the LDR frequency is challenging as it can only be determined through the evaluation of the material response when the tested sample is subject to repeated sweep excitation. Similarly to Fierro et al. [24], [25], a nonlinear narrow sweep excitation (NNSE) with a laser vibrometry system was here used to identify the dual excitation frequencies matching the damage resonance. Particularly, NNSE signals followed by dual periodic excitation were transmitted in order to identify the fundamental frequencies f_1 and f_2 of higher amplitude that generated sidebands and resulted in a higher material nonlinear response with larger temperature gradients across the defect. The layout of the paper is as follows: Section 2 provides the experimental set-up, whilst Section 3 illustrates the identification process of the LDR frequency by means of the NNSE method and dual periodic excitation using the laser vibrometry system. Section 4 reports the

nonlinear wave modulation thermography results and the comparison with flash thermography. Finally, in Section 5, the conclusions about the proposed NWMT inspection technique are discussed.

2 Experimental set-up

The test sample investigated in this work was a CFRP composite panel with a length of 35 cm, width of 25 cm and thickness of 1.3 cm. No further information was provided by the manufacturer about the lay-up and mechanical properties. The specimen was undergone to low-velocity impact at the energy of 20 *J* and BVID was generated approximately in the centre of the panel (marked as the region A on the sample). Figure 1 shows a top view of the CFRP panel and the damaged region using ultrasonic phased array measurements. As it can be seen from Figure 1(b) the extended area of surface delamination is a circular region approximately 2 cm in diameter.

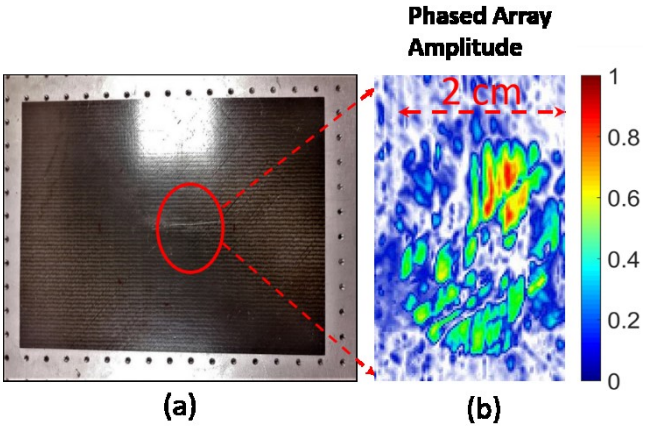

Figure 1. Top view the CFRP sample (a), ultrasonic phased array images of the impact damage based on normalised amplitude measurements (b). As it can be seen from figure (b), the damaged region has a circular shape.

For the ultrasonic signals transmission, a waveform generator (TTi-TGA12104) was connected to two transmitter transducers, i.e. a vacuum Piezoshaker actuator (PS-X-03-6/1000) and a Panametrics narrowband transducer (X1020) with a central frequency of 100 kHz. Both sensors were connected to a high voltage amplifier (Falco Systems WMA-300) in order to increase the output voltage of the

waveform generator. All ultrasonic and thermographic tests were performed at the input voltage of 90 V. Such a level of voltage was chosen to provide a clear nonlinear material response in the damaged composite. Figure 2 shows the position of the transducers relative to the defect location.

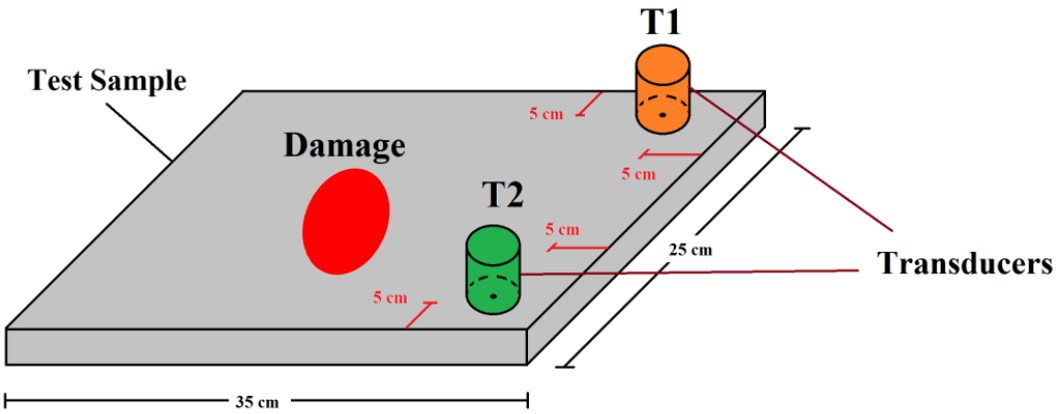

Figure 2. CFRP test sample and location of transmitter transducers. T1 and T2 correspond to the Panametrics X1020 and the Piezoshaker PS-X-03-6/1000 transducers, respectively.

The PSV-500 Polytec 2D laser vibrometer was also used to measure the wave field generated by the dual ultrasonic excitation and to determine the LDR frequency. An indium gallium arsenide IR camera (from FLIR, Merlin) with a frame rate of up to 120 Hz, a resolution of 320 x 256 pixels and a NETD of ~25 mK was employed for the thermographic testing. All thermal measurements were taken at ambient conditions (i.e. ~25°C).

3 LDR determination for Nonlinear Wave Modulation Thermography

The frequency selection process for the actuation of the LDR frequency was divided in two stages. Initially, the NNSE method was used to identify the dual excitation frequencies f_1 and f_2 associated with the LDR effect. Then, both frequencies were simultaneously transmitted as periodic signals in order to focus the elastic energy at the damaged region and generate sidebands and frictional heat at crack location. The position of the two transducers is illustrated in Figure 2.

For the implementation of the NNSE method, three narrowband frequency sweeps with a duration of 72.8 s each were transmitted using the Piezoshaker actuator (see sensor T2 in figure 2). The total

bandwidth ranged between 20 kHz and 40 kHz and three sub-bands were here considered, i.e. 20 - 28 kHz, 28 - 35 kHz and 35 - 40 kHz. The damage-specific resonance frequency f_1 for the dual excitation process was determined by using the highest fundamental amplitudes that, in most cases, generated a high second order nonlinear response $2f_1$. Indeed, a higher harmonic generation indicates that the acoustic wave emitted at the frequency f_1 interacts with the defect, thus confirming the specific resonance nature of damage. At this frequency, the vibration of the defect and the surface temperature gradient above the crack should be higher than any other frequency. Thus, the spectrum from the laser vibrometer was used as a guide for the determination of the optimal excitation. Figure 3 shows the frequency response of the damaged CFRP panel for the three sweep tests measured with the laser vibrometer. Table 1 outlines the fundamental frequencies peaks recorded in each of the three tests.

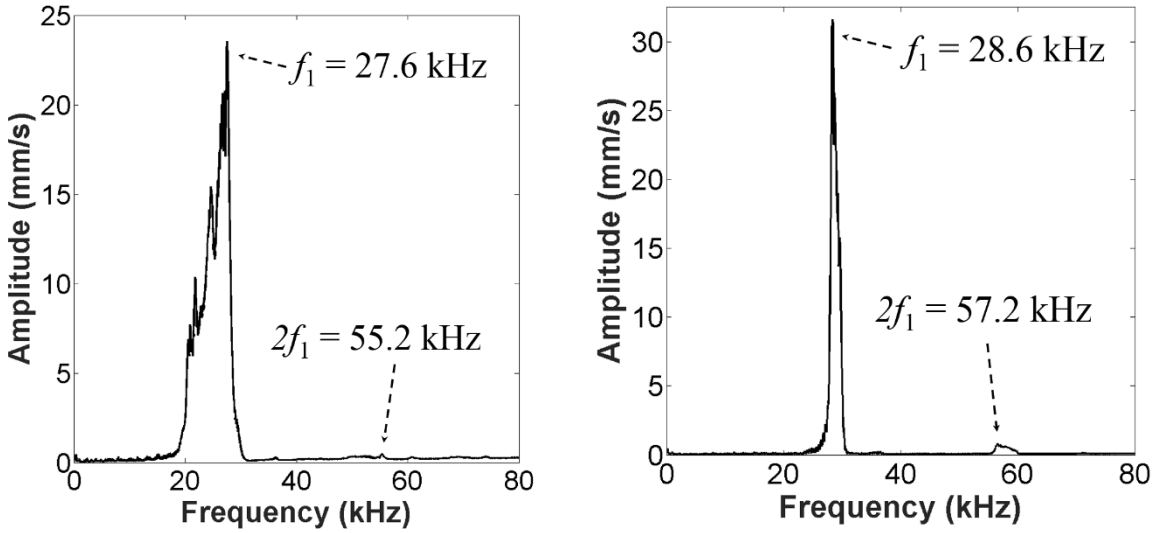

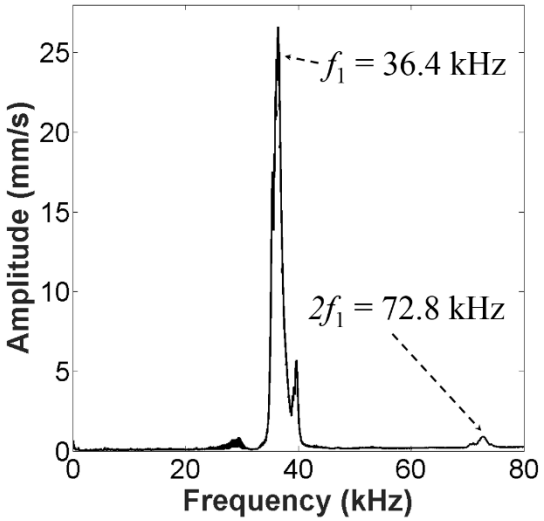

Figure 3. Material nonlinear response measured by the laser vibrometer as a result of the combined continuous signal at the NNSE excitation at three frequency bandwidths: 20-28 kHz (a), 28-35 kHz (b) and 35-40 kHz (c).

Table 1. Selected f_1 frequencies based on the peaks of fundamental amplitudes as in Figure 3.

20-28kHz Sweep (kHz)	**28-35 kHz Sweep (kHz)**	**35-40kHz Sweep (kHz)**
27.56	28.59	36.44

Once the modulation frequency f_1 was selected with the NNSE method, the laser vibrometer was used to evaluate the material response with two simultaneous single tone periodic signals of frequencies f_1 and f_2 applied to the specimen. Unlike both short and chirp pulsed excitation, periodic signals allow focusing the acoustic energy at a single frequency, thus enhancing the generation of nonlinear elastic effects such as sidebands [26], [27], [28]. The time domain signal was captured for a given grid area of the laser vibrometer and the Fast Fourier Transform (FFT) of measured signals was computed to determine the amplitude of both higher harmonics and sidebands. The CFRP panel was excited at different sets of frequencies: the frequency f_2 transmitted with the Panametrics transducer (see sensor T1 in figure 2) was kept fixed at 100 kHz, whilst each of the frequencies reported in Table 1 was tested as the f_1 frequency. The material response for the three frequencies f_1 is shown in Figure 4.

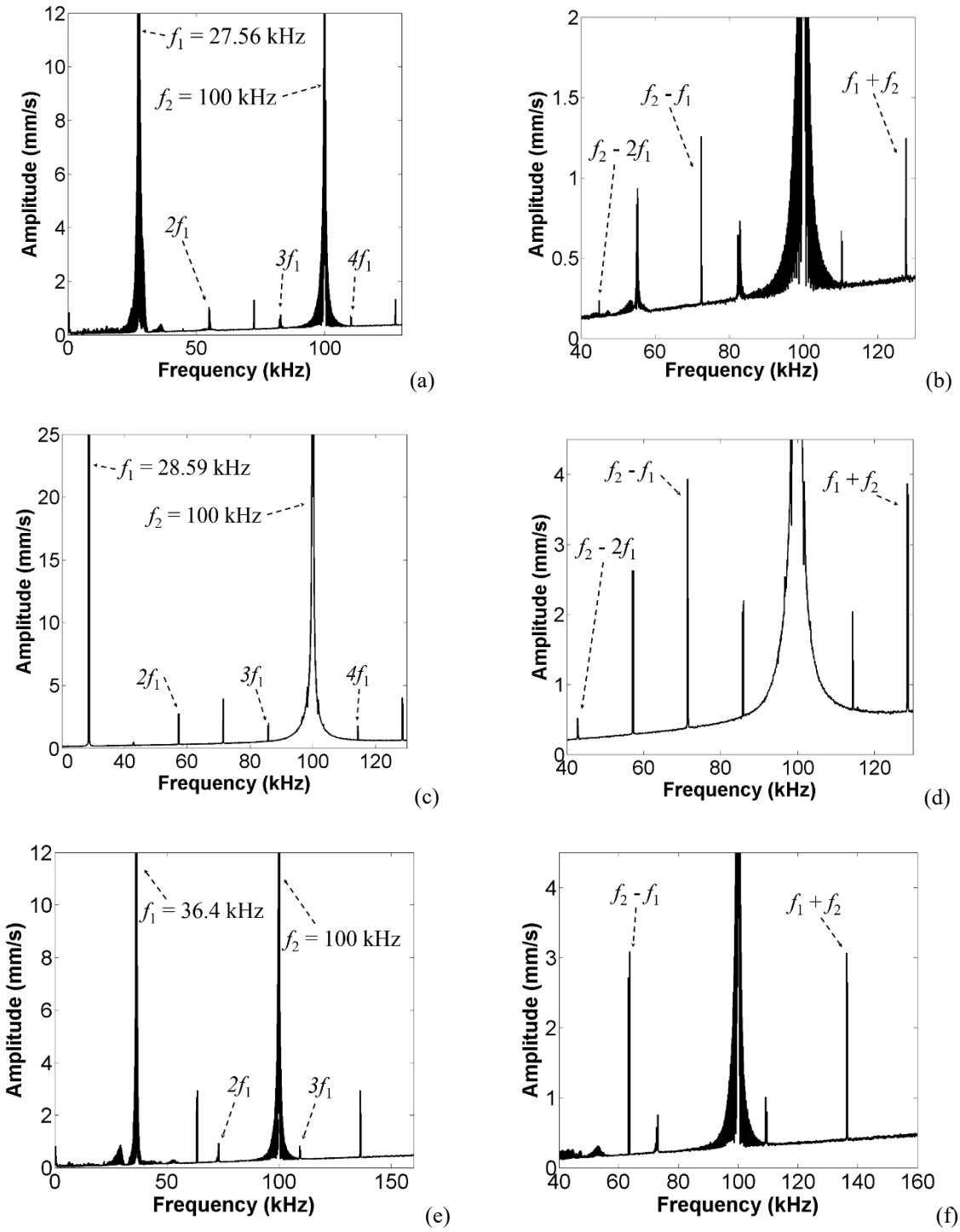

Figure 4. Material frequency response during dual periodic excitation at f_2 = 100 kHz and f_1 = 27.563 kHz (a-b), f_2 = 100 kHz and f_1 = 28.59 kHz (c-d) and f_2 = 100 kHz and f_1 = 36.44 kHz (e-f). The right figures show an enlargement of the corresponding left figure in order to highlight the presence of sidebands f_2-nf_1 and f_2+f_1.

The frequency spectra in Figure 4 showed the generation of higher harmonics and intermodulation products (i.e. sidebands f_2-f_1, f_2-$2f_1$ and f_2+f_1). The spatial mapping of sidebands f_2-f_1 and f_2+f_1 was created using the laser vibrometer in order to identify the location of damage caused by the nonlinear

LDR effect. Figure 5 shows the normalised spatial mapping (i.e. the normalised measured velocity) of sidebands for the input frequency f_1 of 27.6 kHz, 28.6 kHz and 36.4 kHz. Defect location is highlighted by a dashed line in each subfigure.

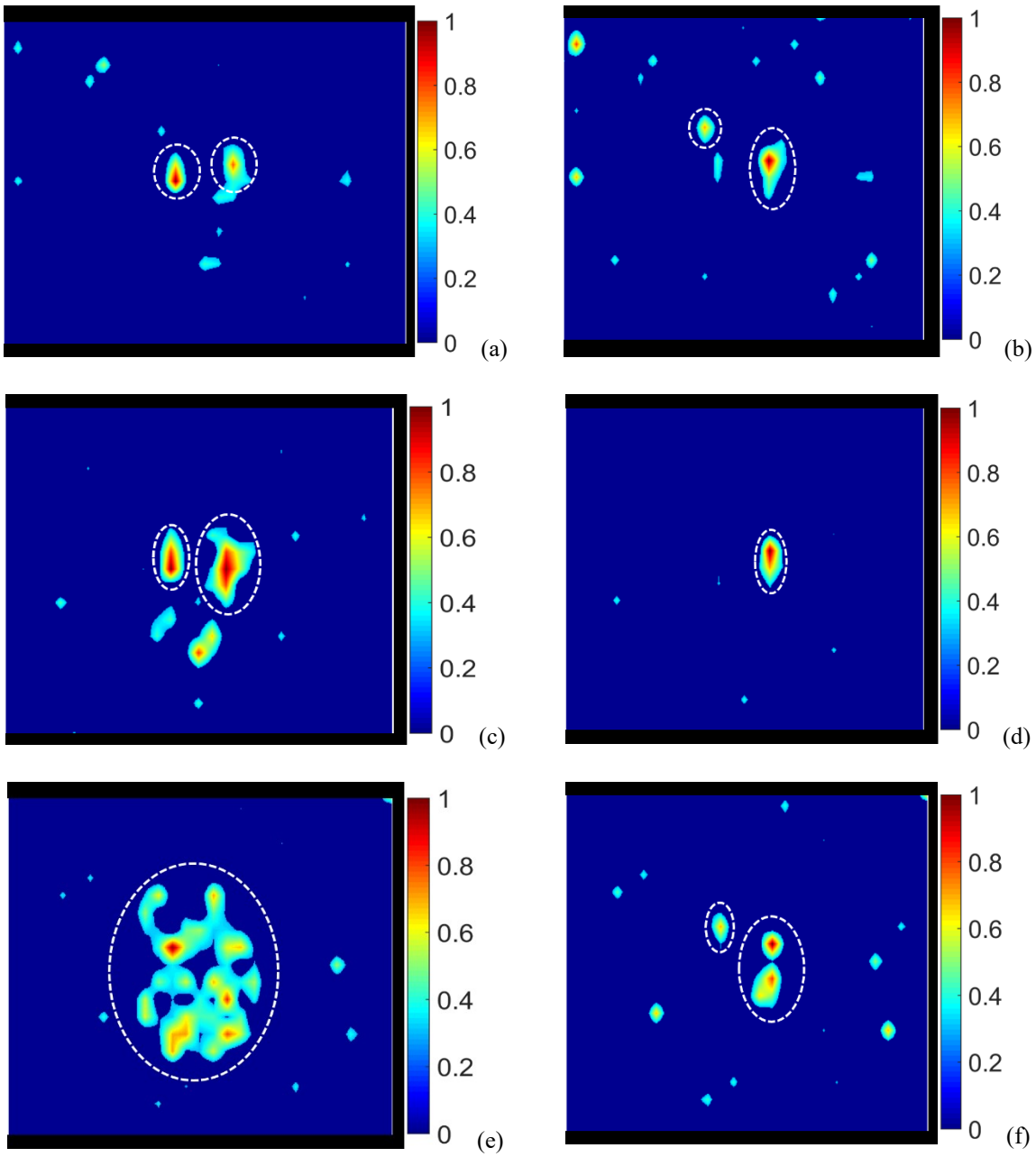

Figure 5. Normalised spatial mapping of f_2-f_1 (left) and f_2+f_1 (right) sidebands in dual modulation excitation – f_1 = 27.563 kHz and f_2 = 100 kHz (a-b), f_1 = 28.594 kHz and f_2 = 100 kHz (c-d), and, f_1 = 36.44 kHz and f_2 = 100 kHz (e-f).

4 Nonlinear wave modulation thermography results

According to Section 3, the damaged CFRP sample was excited at the dual input frequencies f_1 and f_2 that generate high-amplitude intermodulation products. For the thermographic tests, the FLIR IR camera was used to investigate the temperature increase across the defect during ultrasonic excitation. The two piezoelectric transducers were placed at the same position as in Figure 2 in order to transmit ultrasonic periodic waves, whilst thermal data were recorded by the IR camera and post-processed in the PC using a Matlab code.

Initial thermographic testing involved single-frequency excitation only at f_1 and f_2 in order to verify that, for a given input voltage of 90 V, the second harmonic LDR effect of each frequency f_1 and f_2 was lower than the nonlinear elastic response caused by their modulation. The second part of testing included simultaneous dual excitation for ultrasonic wave modulation. The high frequency f_2 was kept fixed at 100 kHz, whereas f_2 was chosen among one of the following frequencies: 27.56 kHz, 28.59 kHz, 32 kHz, and 36.44 kHz. It should be noted that 32 kHz was an arbitrary frequency that, according to Figures 3 and 4, did not cause any significant nonlinear material response during the ultrasonic testing. For each of the following figures, two thermal pictures are reported. The first sub-figure (left) is a raw thermal image, as acquired directly by the camera. The second picture (right) was post-processed with background subtraction and spatial median filtering [29]. For the background subtraction process, the first 100 frames were selected before the ultrasonic excitation and then the average for every pixel across the pre-excitation frames was computed.

a. Comparison of single and dual frequency excitation

In accordance with Figure 3 and Table 1, BVID was successfully detected by exciting the CFRP panel at the single frequency f_1 = 28.594 kHz (see Figure 6). Such a frequency generated second harmonic nonlinear response, which is a sign of interaction of the acoustic wave with the defect, with the highest apparent temperature at damage location of nearly 44 digital levels (Figure 6). Conversely, the single

frequency excitation at f_2 = 100 kHz did not show any heating across the defect (see the apparent temperature images in Figure 7). However, dual frequency excitation has led to a higher temperature difference between the defect and the sound area (Figure 8), with a highest apparent temperature at damage location of 65 digital levels. Figure 9 provides the apparent temperature profile (or IR camera's digital level output) of a pixel within the field of view of the camera at the defect location. As it can be seen in Figure 9, for a given input voltage of 90 V, the temperature rise is significantly higher in the case of dual frequency excitation. This result was already anticipated by the nonlinear ultrasonic tests as the amplitude of sidebands f_2-f_1 and f_2+f_1 was higher than the second harmonic response (see Figure 4). Moreover, the extension of the damage region is in accordance with ultrasonic phased array measurements shown in Figure 1(b) and (c),

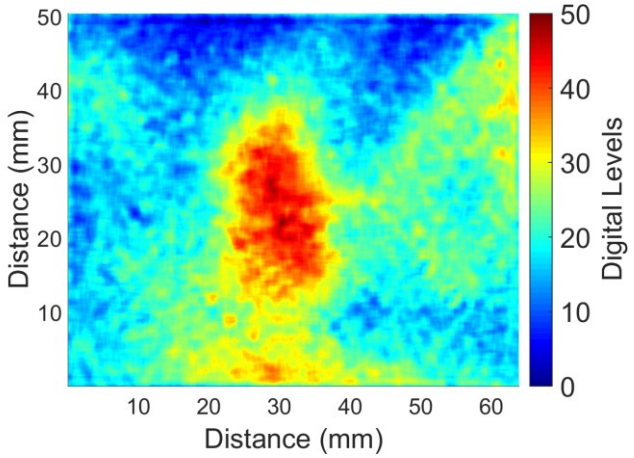

Figure 6. Thermal image of apparent temperature using single periodic excitation at 28.59 kHz. Unit measure is in digital levels measured by the IR camera.

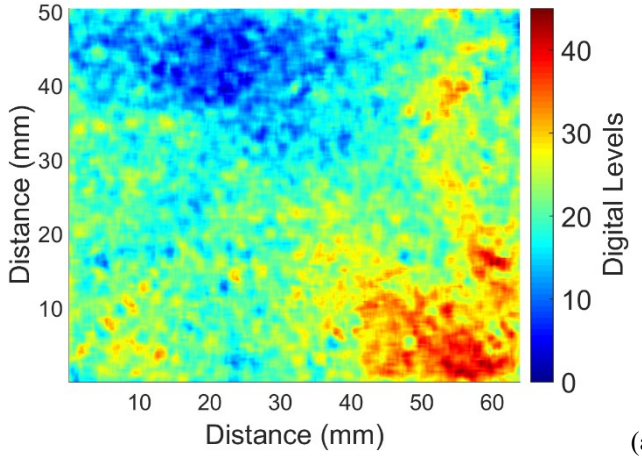

(a)

Figure 7. Thermal image of apparent temperature using single periodic excitation at 100 kHz. Unit measure is in digital levels measured by the IR camera.

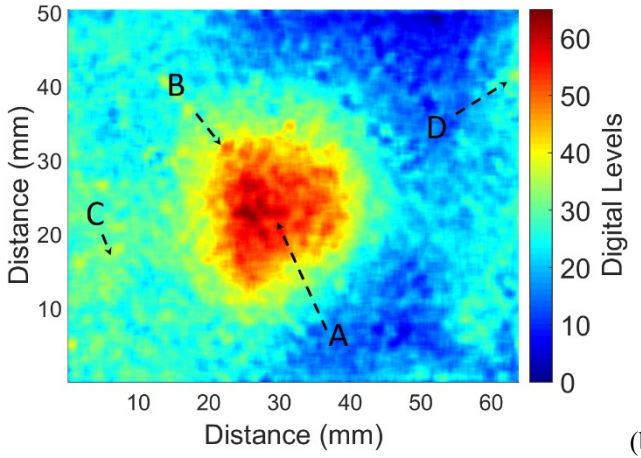

(b)

Figure 8. Thermal image of apparent temperature using dual periodic excitation at 28.59 kHz and 100 kHz. Unit measure is in digital levels measured by the IR camera.

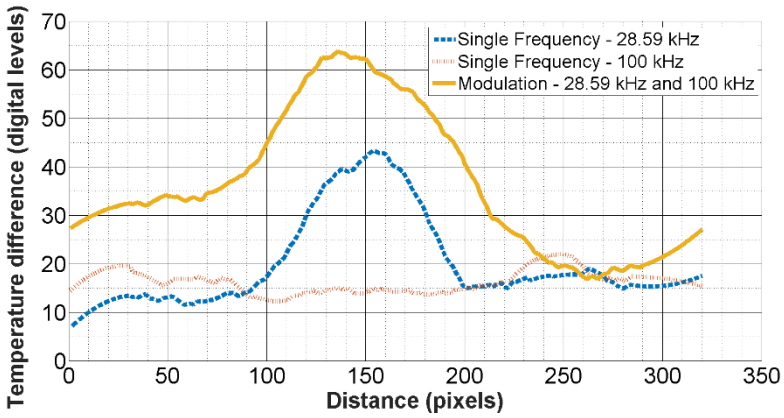

Figure 9. Apparent temperature profile in the x-direction for single and dual frequency excitation.

As illustrated in Figures 8 and 9, BVID was successfully detected with use of the proposed NWMT method. The temperature increase in the centre and in the area around the defect was higher than for any other point further away from it (see Figure 10). Ultrasound testing showed that dual frequency excitation of the test sample at 28.594 kHz and 100 kHz resulted in sidebands of much higher amplitude than in any other case.

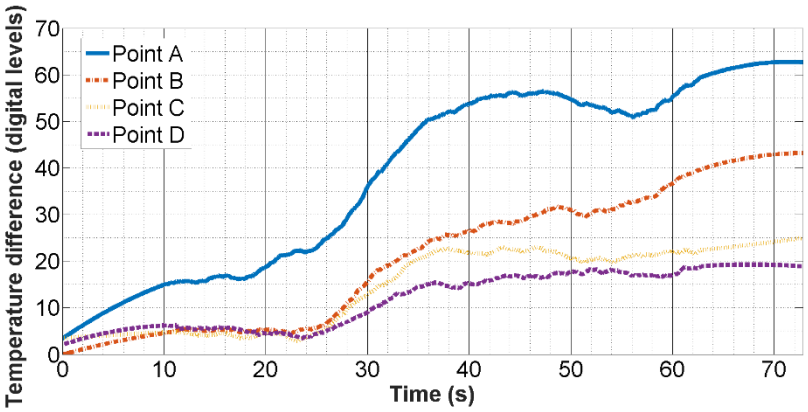

Figure 10. Apparent temperature difference versus time with dual frequency excitation (28.594 kHz and 100 kHz) in the damaged region and the sound area. Please refer to Figure 8 for points A-B-C-D.

The same thermal results were achieved for the other two frequencies f_1 as in Table 1, i.e. 27.563 kHz and 36.44 kHz (see Figures 11 and 12). As expected, during the excitation of the CFRP test sample at 32 kHz, no temperature rise was observed (Figure 13). The apparent temperature evolution for a point in the defect region (here named as point X) for all thermographic tests is reported in Figure 14.

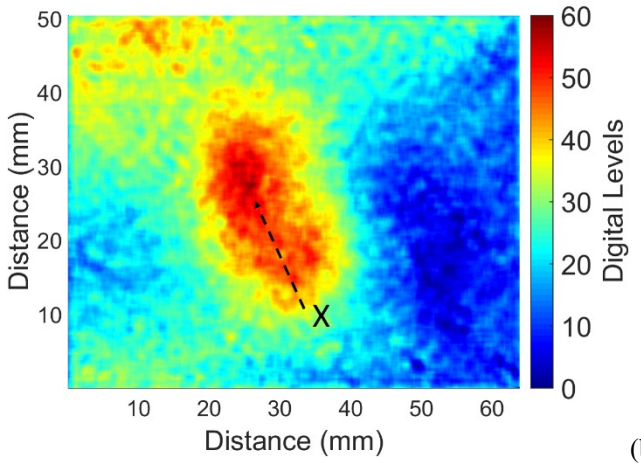

(b)

Figure 11. Thermal image of apparent temperature using dual periodic excitation at 27.563 kHz and 100 kHz. Unit measure is in digital levels measured by the IR camera.

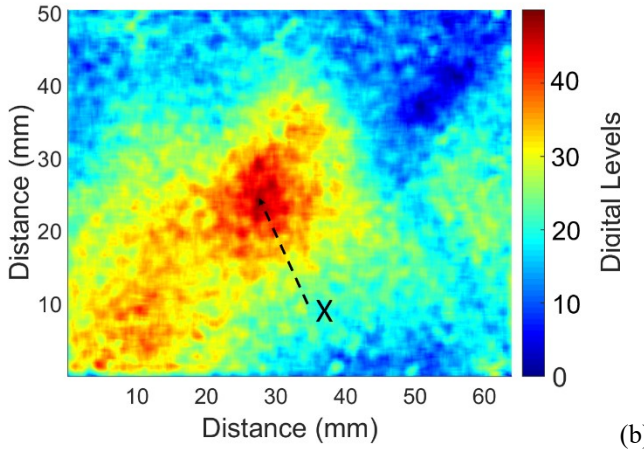

Figure 12. Thermal image of apparent temperature using dual periodic excitation at 36.44 kHz and 100 kHz. Unit measure is in digital levels measured by the IR camera.

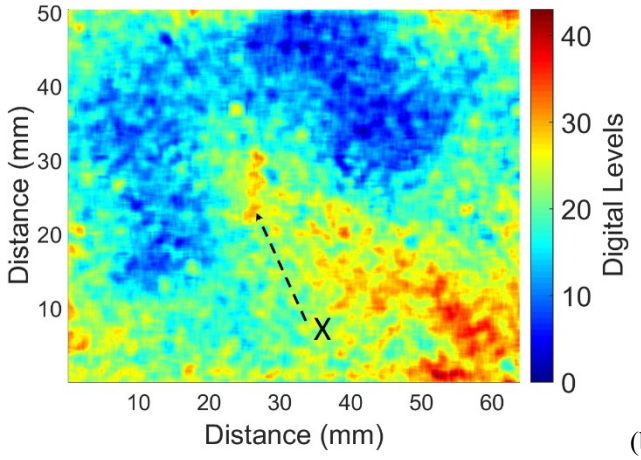

Figure 13. Thermal images of apparent temperature using dual periodic excitation at 32 kHz and 100 kHz. Unit measure is in digital levels measured by the IR camera.

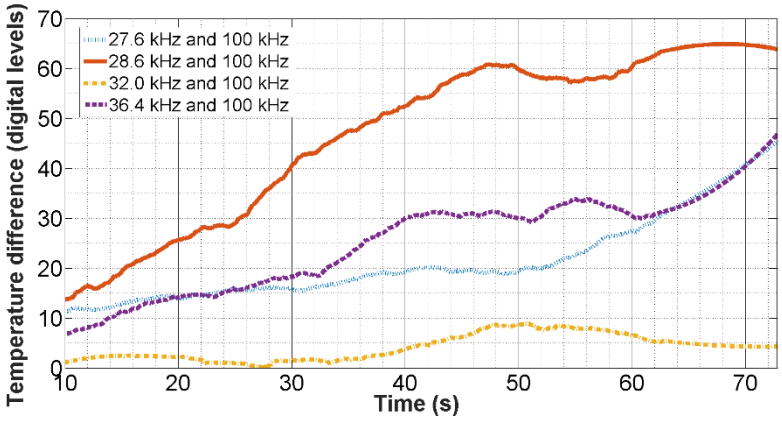

Figure 14. Apparent temperature difference in the damaged region (point X) versus time with dual frequency excitation with NWMT. Please refer to Figures 11, 12 and 13 for the location of point X.

b. Comparison with traditional flash thermography

Flash (or pulsed) thermography was also performed to visualise BVID on the composite sample. A xenon filled quartz flash with a heat input of 3kJ/m^2 and a flash duration of approximately 2 ms was used. The apparent temperature profiles of flash thermography reported in Figures 15 and 16 revealed that only two separate cracks in the damaged area could be observed. Conversely, the proposed NWMT provided high accuracy in imaging the damaged region that, in accordance with the phased array ultrasonic results of Figure 1, it has a circular shape around 2 cm in diameter. This lack of accuracy of flash thermography could be due to the different material responses to thermal excitation in both thermographic techniques. Particularly, whilst the frictional heating caused by local vibrations in NWMT generated sufficient heat along the defect to image the whole damaged area, the lack of air gaps between crack surfaces caused visible heat only in two separate locations (Figure 15) [30]. For this reason, the NWMT method showed a higher level of accuracy in visualising the extended area of subsurface delamination.

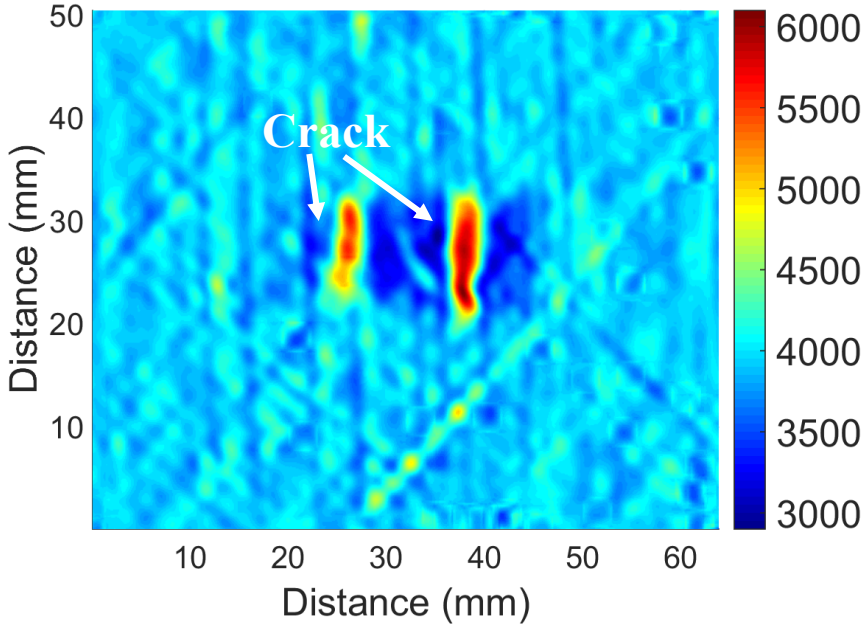

Figure 15. Flash thermography results for defect detection after 9 s.

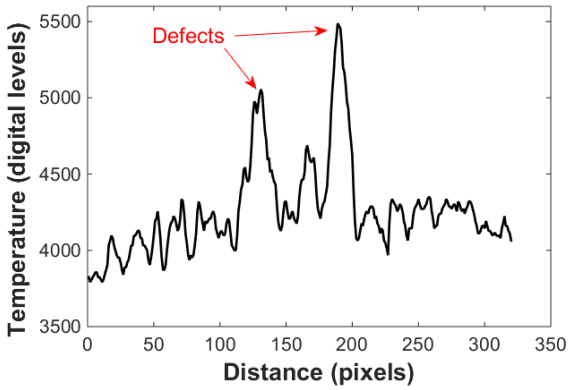

Figure 16. Temperature variations across the x-direction of the tested sample.

5 Conclusion

This paper proposed a novel nonlinear wave modulation thermography (NWMT) technique for effective detection and localisation of BVIDs in composite materials. NWMT initially required narrow sweep excitation in order to identify the excitation frequencies associated with the resonance of the defect. High-amplitude fundamentals and higher harmonic generation are necessary conditions for accurate identification of these frequencies. Dual periodic excitation was then performed in order to generate frictional heating at the crack location that was measured by the IR camera. It has here been shown that the amplitude of a high-frequency wave when modulated with a low-frequency one would give rise to a higher vibrational response that would not be possible through single-frequency excitation. To validate this concept, an impact damaged CFRP panel was tested with the NWMT method and the experimental results were compared to those obtained traditional flash thermography. A laser vibrometer was used to investigate the response of the material with dual frequency excitation and to create a spatial mapping of principal sidebands f_2-f_1 and f_2+f_1 for an accurate defect localisation. The proposed NWMT method is therefore an alternative to traditional thermosonics by allowing repeatable detection of BVID with an accurate visualisation of the extended area of subsurface delamination. The developed nonlinear wave modulation thermography could therefore be considered a reliable and sensitive method for detection of BVIDs in carbon fibre composites.

Acknowledgments

Francesco Ciampa would acknowledge the EPSRC EP/N016386/1 project to support this research work.

References

[1]. Summerscales, J. (Ed.). Non-destructive testing of fibre-reinforced plastics composites (Vol. 2). Springer Science & Business Media, 1990.

[2]. De Francesco, E., De Francesco, R., Leccese, F., Cagnetti, M. A proposal to improve the system life cycle support of composites structures mapping zonal testing data on LSA Databases. 3rd IEEE International Workshop on Metrology for Aerospace, MetroAeroSpace 2016 - Proceedings, art. no. 7573203, pp. 151-155, 2016.

[3]. F. Nanni, S. Nacamulli, R. De Francesco and E. Petritoli, "A new reliability approach for additive layers manufactured components: A preliminary investigation". IEEE International Workshop on Metrology for AeroSpace (MetroAeroSpace), Padua, 2017, pp. 287-290, 2017.

[4]. Almond, D.P, and Pickering, S.G., An analytical study of the pulsed thermography defect detection limit. J. Appl. Phys. 111:093510, 2012.

[5]. Cheng, L., & Tian, G. Y., Surface crack detection for carbon fiber reinforced plastic (CFRP) materials using pulsed eddy current thermography. IEEE Sensors Journals, 11(12), 3261-3268, 2011.

[6]. Morbidini, M, Cawley, P., A calibration procedure for sonic infrared non-destructive evaluation. J. Appl. Phys. 106:023504, 2009.

[7]. Polimeno, U., Almond, D.P., Weekes, B., Chen, E.W.J. A compact thermosonic inspection system for the inspection of composites, Compos Part B: Eng, 59, pp. 67-73, 2014.

[8]. Renshaw, J., Chen, J.C., Holland, S.D., Thompson, R.B. The sources of heat generation in vibrothermography. NDT & E International, 44(8), pp. 736-739, 2011.

[9]. Blau, P.J., Friction science and technology: from concepts to applications. CRC press, 2008.

[10]. Morbidini, M., Kang, B., Cawley, P. Improved reliability of sonic infrared testing. Materials Evaluation, 67(10), pp. 1193-1202, 2009.

[11]. Sohn, H., Lim, H. J., DeSimio, M.P., Brown, K., & Derriso, M. Nonlinear ultrasonic wave modulation for online fatigue crack detection. Journal of Sound and Vibration, 333(5), pp. 1473-1484, 2014.

[12]. Kober, J., & Prevorovsky, Z. Theoretical investigation of nonlinear ultrasonic wave modulation spectroscopy at crack surface. NDT & E International, 61, pp. 10-15, 2014.

[13]. Donskoy, D. M., & Sutin, A. M. Vibro-Acoustic Modulation Nondestructive Evaluation Technique. Journal of Intelligent Material Systems and Structures, 9(9), pp. 765-771, 1998.

[14]. Fierro, G. P. M., & Meo, M. Residual fatigue life estimation using a nonlinear ultrasound modulation method. Smart Materials and Structures, 24(2), 025040, 2015.

[15]. Ciampa, F., Barbieri, E., Meo, M. Modelling of Multiscale Nonlinear Interaction of Elastic Waves with Three Dimensional Cracks. Journal of Acoustical Society of America, 135(4), 2014.

[16]. Fierro, G. P. M., & Meo, M. Nonlinear imaging (NIM) of flaws in a complex composite stiffened panel using a constructive nonlinear array (CNA) technique. Ultrasonics, 74, 30-47, 2017.

[17]. Meo, M., Polimeno, U., Zumpano, G., Detecting damage in composite material using nonlinear elastic wave spectroscopy methods. 15(3), pp. 115-126, 2008.

[18]. De Angelis, G., Dati, E., Bernabei, M., Leccese, F. Development on aerospace composite structures investigation using thermography and shearography in comparison to traditional

NDT methods. 2nd IEEE International Workshop on Metrology for Aerospace, MetroAeroSpace 2015 - Proceedings, art. no. 7180625, pp. 49-55, 2015.

[19]. Angelis, G. D., Meo, M., Almond, D. P., Pickering, S. G., Angioni, S. L. A new technique to detect defect size and depth in composite structures using digital shearography and unconstrained optimization. NDT & E International, 45, pp. 91-96, 2012.

[20]. Solodov, I. Resonant acoustic nonlinearity of defects for highly-efficient nonlinear NDE. Journal of Nondestructive Evaluation, 33(2), pp. 252-262, 2014.

[21]. Solodov, I. Local defect resonance (LDR): A route to highly efficient thermosonic and nonlinear ultrasonic NDT. In AIP Conference Proceedings edited by Dale E. Chimenti, Leonard J. Bond, and Donald O. Thompson, 1581(1), pp. 1663-1670, 2014.

[22]. Solodov, I., Bai, J., Bekgulyan, S., & Busse, G. A local defect resonance to enhance acoustic wave-defect interaction in ultrasonic non-destructive evaluation. Applied Physics Letters, 99(21), 211911, 2011.

[23]. Solodov, I., Bai, J., & Busse, G. Resonant ultrasound spectroscopy of defects: case study of flat-bottomed holes. Journal of Applied Physics, 113(22), 223512, 2013.

[24]. Fierro, G.P.M., Ginzburg, D. Ciampa, F., Meo, M. Nonlinear ultrasonic stimulated thermography for damage assessment in isotropic fatigued structures. Journal of Sound and Vibration, 404, 102-115, 2017.

[25]. Fierro, G.P.M., Ginzburg, D., Ciampa, F., Meo, M. Nonlinear thermosonics and laser vibrometry for barely visible impact damage for a composite stiffener panel. In SPIE 9804, Nondestructive Characterization and Monitoring of Advanced Materials, Aerospace, and Civil Infrastructure, 980419 (April 22, 2016), 2016.

[26]. Kazakov, V.V., Sutin, A., & Johnson, P.A. Sensitive imaging of an elastic nonlinear wave-scattering source in a solid. Applied Physics Letter, 81(4), pp.646-648, 2002.

[27]. Ciampa, F., Scarselli, G., Pickering, S., Meo, M. Nonlinear imaging of damage in composite structures using sparse ultrasonic sensor arrays. Structural Control and Health Monitoring, 24(5), 2017.

[28]. Ciampa, F., Scarselli, G., Pickering, S., Meo, M. Nonlinear elastic wave tomography for the imaging of corrosion damage. Ultrasonics, 62, pp. 147-155, 2015.

[29]. Pinto, F., Ciampa, F., Meo, M., Polimeno, U. Multifunctional SMART composite material for in situ NDT/SHM and de-icing. Smart Materials and Structures, 21(10), 105010, 2012.

[30]. Shepard, S.M., Hou, Y., Ahmed, T., & Lhota, J.R. Reference-free interpretation of flash thermography data. Insight-Non-Destructive Testing and Condition Monitoring, 48(5), pp. 298-301, 2006.